Available online at www.sciencedirect.com
SCIENCE DIRECT
Physics Letters A 356 (2006) 72–78
PHYSICS LETTERS A
www.elsevier.com/locate/pla

Ignition regime for fusion in a degenerate plasma

S. Son *, N.J. Fisch

Department of Astrophysical Sciences, Princeton University, Princeton, NJ 08540, USA

Received 29 November 2005; received in revised form 15 February 2006; accepted 28 March 2006

Available online 17 April 2006

Communicated by F. Porcelli

Abstract

We identify relevant parameter regimes in which aneutronic fuels can undergo fusion ignition in hot-ion degenerate plasma. Because of relativistic effects and partial degeneracy, the self-sustained burning regime is considerably larger than previously calculated. Inverse bremsstrahlung plays a major role in containing the reactor energy. We solve the radiation transfer equation and obtain the contribution to the heat conductivity from inverse bremsstrahlung.

PACS: 52.25.Fi; 52.57.Kk; 71.10.Ca

Keywords: Aneutronic; Fusion; Degeneracy; Stopping; Bremsstrahlung; Proton; Boron; Helium; Deuterium

1. Introduction

It would be desirable to achieve controlled thermonuclear reaction that produces the fewest neutrons or no neutrons. The most promising fuel with no neutron (sometimes called advanced fuel) is proton–boron-11 [$P+B^{11} \rightarrow 3\alpha(2.7\,\mathrm{MeV})$] and deuterium–helium-3 [$D+He^3 \rightarrow p(14.7\,\mathrm{MeV})+\alpha(3.6\,\mathrm{MeV})$]. However, in classical plasmas, self-burning of advanced fuels is unlikely [1], because, at high temperatures, it seems that the bremsstrahlung loss may exceed the fusion power produced.

In Fermi degenerate plasmas, the prospect of the aneutronic fuel burning can be very different due to the reduction of ion–electron (i–e) collisions, which both allows the ion temperature to exceed the electron temperature and reduces the bremsstrahlung loss. In previous work [2,3], it was showed that the fusion byproducts can be stopped primarily not by electrons but by ions, thus allowing a regime of operation in which ions are hotter than electrons, the so-called "hot-ion mode" of operation. This occurs when the density is more than $n_e = 10^{29}\ \mathrm{cm}^{-3}$; self-sustained burning is then achieved where the ion temperature is more than 100 keV and the electron temperature is 30 keV. This regime has more favorable energy balance than the equal temperature mode, and so can enable the self-sustained burning of aneutronic fuel. The reduction of the i–e collisions can be also applied to D–T burning to achieve high ion and low electron temperature. While much effort can be expended to realize the hot-ion mode in conventional magnetic fusion [4–6], in degenerate plasmas, such an effort is not needed, where the hot-ion mode occurs "naturally". Also, a related effect is that in the degenerate plasma regime, the reduction in e–i collisions relative to classical plasma increases the current drive efficiency [7].

Previous calculations of the fusion ignition regime [2,3] ignored the effects of partial degeneracy and the relativistic effects on the i–e collisions, the reduction of the bremsstrahlung, and the fraction of energy that goes from fusion byproducts into electrons, which are now available [8]. In this Letter, we use these result [8] to quantify more accurately the regime for fusion burning, showing that the self-sustained burning regime of advanced fuel is several times larger than the previous result [2]. Recently Leon et al. [9] showed that plasma degeneracy lower the ignition temperature for D–T, and that for P–B-11, the ignition temperature can be lower than 20 keV when $\rho = 3.3 \times 10^7\ \mathrm{g/cm}^3$. We show that the density condition can be

* Corresponding author.
E-mail addresses: sson@pppl.gov (S. Son), fisch@pppl.gov (N.J. Fisch).

0375-9601/$ – see front matter
doi:10.1016/j.physleta.2006.03.065

eased further. We also solve ρR-equation in the inertial confinement fusion and determine the pellet dimension. Furthermore, we show that inverse bremsstrahlung is much more efficient than the Compton effect in the re-absorption so that the fuel is optically thick.

This Letter is organized as follows. In Section 2, based on [8], we identify the self-burning regime of the aneutronic fuel, and solve a 0D power balance equation to show that burning is feasible. In Section 3, we solve ρR equation. In Section 4, we consider various aspects of the re-absorption mechanism and show that the fuel re-absorbs photons via the inverse bremsstrahlung. In Section 5, a summary and conclusion are given.

2. Regimes of self-burning in a degenerate plasma

In previous work [2], we showed that the optimal fuel concentration, $\epsilon = n_B/n_p$, is 0.3 and the electron density should be larger than $n_0 = 6.69 \times 10^{28}$ $(1/\mathrm{cm}^3)$ for self-burning of P–B-11. For an example, when $n_e = 2n_0$ (the Fermi energy $E_F = 95$ keV), we showed that $T_e = 27$ keV when $T_i = 200$ keV. In the D–He-3 case, we showed that as an example, for $\rho = 3 \times 10^5$ $(\mathrm{g/cm}^3)$ ($E_F = 90$ keV) and $n_D/n_{He} = 0.1$, $T_e = 35$ keV when $T_i = 70$ keV for self-burning. However, this calculation was made using the classical bremsstrahlung formula and zero electron temperature stopping frequency without relativistic corrections and partial degeneracy effects.

In our recent work [8], we apply the work on the stopping [10,11] to show how the partial degeneracy can change the stopping in our particular regime. We also show that the relativistic effects reduce the electron stopping by 10–20%, which agree well with Nagy [12]. We then show how the partial degeneracy and the relativistic effects can change the prediction about the fraction of energy that goes from fusion by-products into electrons. We show in this section how these effects ignored will expand the self-burning regime further.

2.1. 0D power balance equation

We now integrate, numerically in time, the fuel evolution using the reduction formula in radiation and stopping power from [8]. We assume that the fuel is homogeneous in space. The densities and temperatures of electrons and ions are governed by the following equations [13]:

$$\begin{aligned}
&\frac{3}{2}n_e\frac{dT_e}{dt} = P_{ie} - P_B + \eta(T_e)P_F,\\
&(\Sigma_i n_i)\frac{3}{2}\frac{dT_i}{dt} = -P_{ie} + \big[1-\eta(T_e)\big]P_F,\\
&\frac{dn_1}{dt} = -n_1 n_2\langle\sigma v\rangle,\\
&\frac{dn_2}{dt} = -n_1 n_2\langle\sigma v\rangle,\\
&\frac{dn_F}{dt} = n_1 n_2\alpha_F\langle\sigma v\rangle. \qquad (1)
\end{aligned}$$

The bremsstrahlung losses, P_B, is given in [14]; the fusion power, P_F, is given in [15]; η, which was analyzed in [8], is the fraction of energy that goes from fusion byproducts into electrons; the densities of fusing-ion species are n_1 and n_2; the density of the fusion by-product is n_F; we define α_F as the number of F-particles per fusion; the energy input from ions to electrons via Coulomb collisions, P_{ie}, is given by $P_{ie} = (\Sigma_i n_i Z_i/m_i)(8/3\pi(e^4 m_e^2/\hbar^3))C(T_e)(3T_i/2)$ (for the definition of $C(T_e)$, look [8]).

By normalizing the above equation (the density by the electron density n_e, the temperature by the Fermi energy E_F, and the time by the stopping time $1/\tau_s = (8/3\pi)(m_e^2 e^4/\hbar^3 m_n)$, where m_n is the mass of a neutron), we can simplify Eq. (1) in a dimensionless variables.

$$\begin{aligned}
\frac{d\theta_e}{ds} &= \big(\Sigma_i\tilde{n}_i Z_i^2/m_i\big)C(\theta_e)\theta_i - \beta\big(\Sigma_i\tilde{n}_i Z_i^2\big)f(T_e)\\
&\quad + \frac{2}{3}\eta(\theta_e)\tilde{n}_1\tilde{n}_2\frac{\Delta E}{E_F}\gamma(\theta_i),\\
\frac{d\theta_i}{ds} &= \left(\frac{\Sigma_i\tilde{n}_i Z_i^2/m_i}{\Sigma_i\tilde{n}_i}\right)C(\theta_e)\theta_i + \frac{2}{3}\big[1-\eta(\theta_e)\big]\frac{\Delta E}{E_F}\frac{\tilde{n}_1\tilde{n}_2}{\Sigma_i\tilde{n}_i}\gamma(\theta_i),\\
\frac{d\tilde{n}_1}{ds} &= -\tilde{n}_1\tilde{n}_2\gamma(\theta_i),\\
\frac{d\tilde{n}_2}{ds} &= -\tilde{n}_1\tilde{n}_2\gamma(\theta_i),\\
\frac{d\tilde{n}_F}{ds} &= +\alpha_F\tilde{n}_1\tilde{n}_2\gamma(\theta_i), \qquad (2)
\end{aligned}$$

where $\tilde{n}_i = n_i/n_e$, $\theta_i = T_i/E_F$, $\theta_e = T_e/E_F$, $\beta = (8\pi/9)(e^2/\hbar c)^3(m_n\hbar^2 E_f/m_e^2 e^4)$, $C(\theta_e)$, $f(\theta)$ is given in [8], ΔE is the energy produced per fusion, and $\gamma(T_i) = n_e\langle\sigma v\rangle(3\pi/8)(\hbar^3 m_n/m_e^2 e^4)$. The same analysis can be performed for the D–He-3 fuel. We do not repeat the analysis. However, the result of the numerical computation is presented in the next section.

2.2. 0D power balance for the P–B-11

In Fig. 1, we show the time integration of the electron and the ion temperature, the remaining fraction of Boron fuel for $n_e = 4\times 10^{28}$ cm^{-3} ($E_F = 43$ keV) with the initial condition of $T_e = 0$, $T_i = 200$ keV and $n_B/n_P = 0.25$. We also plot the fraction of energy from fusion byproducts to electrons as a function of time. Initially, the ion temperature decreases in time: the fusion power is less than the energy dissipation from ions into electrons. The electron temperature increases in time because electrons cannot radiate the energy input from ions fast enough since the bremsstrahlung is much smaller than the classical prediction. As electron temperature increases, i–e collisions decrease, and energy transfer from ions then decreases. Thus, fusion power becomes higher than energy dissipation from ions to electrons, and ion temperature increases. As shown, the maximum of electron temperature matches with the minimum of the fraction of energy from fusion byproducts into electrons. According to previous work [2], since n_e is the below the critical density n_0, there is no self-burning regime. However, in that analysis, the partial degeneracy, the relativistic effect in the stopping power, and the reduction of the bremsstrahlung losses are entirely ignored. As shown in the figure, the fuel is self-burning due to the fact that those ignored factor eases the

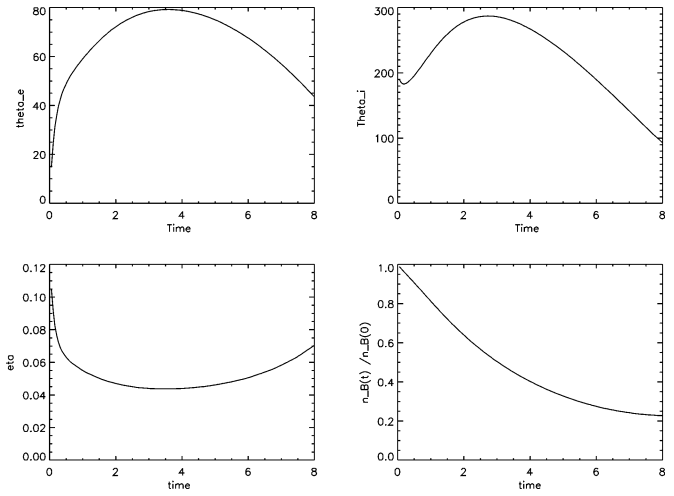

Fig. 1. The time integration of electron and ion temperature, the remaining fraction of Boron fuel for $n_e = 4 \times 10^{28}$ cm^{-3} ($E_F = 43$ keV) with the initial condition $T_e = 0$, $T_i = 200$ keV and $n_B/n_P = 0.25$. Top left: the electron temperature (Y-axis: the temperature in keV, X-axis: the time in the unit of 0.5×10^{-13} s). Top right: the ion temperature (Y-axis: the temperature in keV, X-axis: the time in the unit of 0.5×10^{-13} s). Bottom left: the fraction of energy from an alpha particle to electrons (Y-axis: r_e, X-axis: the time in the unit of 0.5×10^{-13} s). Bottom right: the fraction of remaining boron fuel $n_B(\tau)/n_B(0)$.

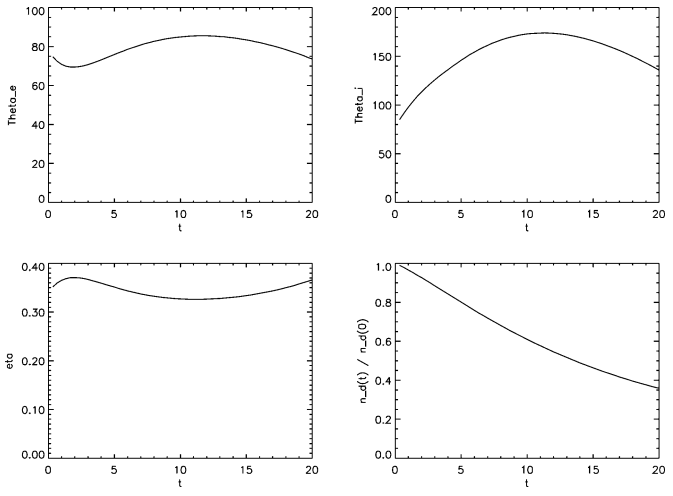

Fig. 2. The time integration of electron and ion temperature, the remaining fraction of deuterium fuel for $n_e = 10^{28}$ cm^{-3} ($E_F = 17$ keV) with the initial condition $T_e = 78$ keV, $T_i = 78$ keV and $n_d/n_{he} = 0.1$. Top left: the electron temperature (Y-axis: the temperature in keV, X-axis: the time in the unit of 0.5×10^{-13} s). Top right: the ion temperature (Y-axis: the temperature in keV, X-axis: the time in the unit of 0.5×10^{-13} s). Bottom left: the fraction of energy from an alpha particle to electrons (Y-axis: r_e, X-axis: the time in the unit of 0.5×10^{-13} s). Bottom right: the fraction of remaining boron fuel $n_D(\tau)/n_D(0)$.

condition further. For too large or too low ϵ, the fuel will not burn due to the severe radiation losses. We can show that, for this density, ϵ must be $0.2 < \epsilon < 0.4$ for the fuel to be self-burning.

2.3. 0D power balance equation for the D–He-3

In Fig. 2, we show the same set of 0D power balance equation for $n_e = 10^{28}$ cm^{-3} ($E_F = 16.9$ keV) with the initial condition of $T_e = 78$, $T_i = 78$ keV and $n_d/n_{he} = 0.1$. Due to the reduction of the i–e collisions, the fuel is self burning, and ion temperature reaches 200 keV.

In Fig. 3, we show the same set of 0D power balance equation for $n_e = 4 \times 10^{27}$ cm^{-3} ($E_F = 9$ keV) with the initial condition of $T_e = 78$ keV, $T_i = 78$ keV and $n_d/n_{he} = 0.1$. As shown, the fuel is self-burning. However, because E_F is comparable to the initial proton energy divided by electron–proton mass ratio, the assumption $v_F \gg v$ (v is proton velocity) is not valid and there can be 100% errors in i–e collision rate. However, this computation suggests that D–He-3 can be burn for the density $\rho \cong 10^4$ g/cm^3 and the temperature $T_i \cong 100$ keV.

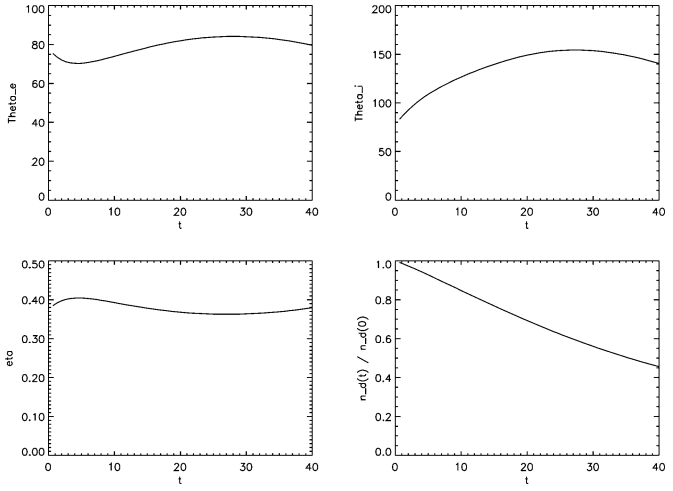

Fig. 3. The time integration of electron and ion temperature, the remaining fraction of deuterium fuel for $n_e = 4 \times 10^{27}$ cm^{-3} ($E_F = 9$ keV) with the initial condition $T_e = 78$ keV, $T_i = 78$ keV and $n_d/n_{he} = 0.1$. Top left: the electron temperature (Y-axis: the temperature in keV, X-axis: the time in the unit of 0.5×10^{-13} s). Top right: the ion temperature (Y-axis: the temperature in keV, X-axis: the time in the unit of 0.5×10^{-13} s). Bottom left: the fraction of energy from an alpha particle to electrons (Y-axis: r_e, X-axis: the time in the unit of 0.5×10^{-13} s). Bottom right: the fraction of remaining boron fuel $n_D(\tau)/n_D(0)$.

3. ρR equation and pellet dimension

To find the pellet dimension and total power, we solve the ρR equation (for a review, see [16]) in the P–B-11 with $\epsilon = 0.3$ and $\rho = 2.0 \times 10^5$ (g/cm^3):

$$\frac{dx}{dt} \cong n_p \langle \sigma v \rangle x(0.7 + x), \tag{3}$$

where x is the ratio of the deuterium density to the initial helium density; $x = 0.3$ at $t = 0$, and $x = 0$ at total burn-up. The solution is $x/(0.7 + x) \cong 0.3 \exp(-t n_p \langle \sigma v \rangle)$. For the total burn-up, the confinement time $t_c = R/C_s$ must be longer than $1/n_p \langle \sigma v \rangle \cong 0.5 \times 10^{-13}$ s, where C_s is the sound wave velocity, and R is the pellet dimension. Assuming $C_s \cong \sqrt{nE_F/\rho}$, then R must be larger than 10^{-4} cm. In a conventional ρR equation: $f = \rho R/(\rho R + \beta)$, where f the burn fraction, and $\beta = 3MC_s/\langle \sigma v \rangle$. We can estimate that for the D–He-3 or the P–B-11, $\beta \cong 25$–50 g/cm^2. For the P–B-11 case, by compressing a pellet to a state with $\rho \cong 10^5$ g/cm^3 and the ra-

dius $R \cong 0.002$ cm, the input at the electron Fermi energy is 4 MJ and the output will be 160 MJ. In this case, the confinement time is estimated longer than a picosecond and is long enough. For the D–He-3 case, by compressing a pellet to a state with $\rho = 10^4$ g/cm^3, and the radius $R = 0.01$ cm, the input at the electron Fermi energy is 7 MJ, and output energy will be 600 MJ. In this case, the confinement time can be estimated to be longer than a picosecond and is long enough. The feasibility as a reactor for either of these fuels is low because the gain is smaller than 100. The gain is 10 times smaller than D–T fuel. We note that the gain can be as large as 1000 in D–T fuel [16].

4. Radiation re-absorption

The radiated photons are absorbed mainly via the inverse bremsstrahlung or the Compton processes. Eliezer [13] has shown that, in some regime with a particular temperature range, the Compton process dominates the inverse bremsstrahlung. We show in this section that the opposite is true in our regime. For this, we develop the Green's function approach and calculate the heat conductivity due to photon-induced transfer.

4.1. Compton effect

In the reference frame in which a electron is at rest, the Compton scattering cross section is given by the Klein–Nishina formula as

$$\frac{d\sigma_{\mathrm{KN}}}{d\Omega} = \frac{r_0^2}{2}\frac{\epsilon_1^2}{\epsilon^2}\left(\frac{\epsilon_1}{\epsilon} + \frac{\epsilon}{\epsilon_1} - \sin^2\Theta\right), \tag{4}$$

where $\sigma_T = 8\pi/3r_0^2 = 6.65 \times 10^{-25}$ cm^2 is the Thomson cross section, and ϵ (ϵ_1) is the initial (final) photon energy. The relationship among ϵ_1, ϵ and Θ is given as $\epsilon_1 = \epsilon/[1 + (\epsilon/m_e c^2)(1 - \cos\Theta)]$. If $\epsilon \ll m_e c^2$, then $\epsilon_1 \cong \epsilon$ and the cross-section becomes the Thomson elastic cross section. By integrating Eq. (4) over the solid angle, the total Klein–Nishina cross section can be obtained as

$$\sigma_{\mathrm{KN}} = +\frac{3}{4}\frac{1+x}{x^3}\left[\frac{2x(1+x)}{1+2x} - \log(1+2x)\right] + \frac{1}{2x}\log(1+2x) - \frac{1+3x}{(1+2x)^2}, \tag{5}$$

where $x = \hbar\nu/m_e c^2$. In non-relativistic regime ($x \ll 1$), it can be simplified as $\sigma = \sigma_T[1 - 2x + (26/5)x^2]$.

Let us now estimate how much a photon travels before most of its energy is re-absorbed by electrons. If the photon energy is small compared with the rest mass, the average energy absorbed per a Compton scattering can be estimated as $\epsilon(\epsilon/m_e c^2)$ from Eq. (5). The energy equations for the photon can then be written as $(d\epsilon/dt) = -n_e\sigma_T c(\epsilon/m_e c^2)\epsilon$, whose solution is $\epsilon(t) = 1/(1 + t/\tau_C)$ with $1/\tau_C = (n_e\sigma_T c)(\epsilon_0/m_e c^2)$, where ϵ_0 is the initial energy of the photon. At $t = t_{1/2} = \tau_C$, the half of the photon's energy is re-absorbed by electrons. The distance traveled by a photon during $t = t_{1/2}$ can be estimated as follows. The photon traveling can be considered as the random work (at each collision, the photon reduces its energy by small amount and changes its direction randomly). Then, the photon position can be obtained as a solution of the simple diffusion equation, whose solution is a Maxwellian with only one undetermined parameter (standard deviation L). Since the average time interval between the scattering is $\tau_n \cong 1/n_e\sigma_T c$, the diffusion coefficient D can be estimated as $D \cong c^2 t_n$ (assuming the photon is scattered isotropically). Then, at $t = t_{1/2}$, the root-mean square of the distance that the photon has traveled can be estimated as $L \cong \sqrt{Dt_{1/2}} = (1/n_e\sigma_T)\sqrt{m_e c^2/\epsilon(0)}$. We can easily see that the less energetic the photon is, the more distance it travels before it loses half of its energy. As an example, for electron density $n_e = 10^{29}$ cm^{-3}, we obtain $L \cong 10^{-4}$ cm for a 10 keV photon. However, the actual L is much larger than the result because the Compton scattering is much reduced from the degeneracy.

4.2. Inverse bremsstrahlung

Inverse bremsstrahlung has been calculated classically by Dawson and Oberman [17], then by Silin [18]. Later, Seely and Harris [19] calculated one-photon and multi-photon process using the Born approximation and found that the result matches the result by Dawson and Oberman [17]. The multi-photon process of inverse bremsstrahlung is refined later by a few authors [20,21]. We use some of the result from Shima and Yatom [20].

The one-photon process in completely degenerate plasma and partially degenerate plasma has been presented in [20]. In this section, we assume the complete degeneracy. From Shima's result, we write the absorption formula of one-photon process in laser field as

$$\frac{dW}{dt} = 2\pi n_i Z_i^2 n_e m_e \left(\frac{eE}{m_e\omega}\right)^2 \left(\frac{e^4}{m_e^2 v_F^3}\right)\log\left(\frac{1}{q}\right), \tag{6}$$

where W is in the units of eV/cm^3, v_F is the Fermi energy, ω is the laser frequency, E is the electric field strength of the laser, and $q = \hbar\omega/2m_e v_F^2$. Note that the electric field and photon density can be related as $n_p\hbar\omega = (E^2/8\pi)$, where n_p is the number of photon per volume. Using this, we can obtain the inverse bremsstrahlung time scale as

$$\nu_i(\omega) = 4\pi n_i Z_i^2 \left(\frac{e^4}{m_e^2 v_F^4}\right) v_F \log\left(\frac{1}{q}\right)\frac{\omega_{pe}^2}{\omega^2}. \tag{7}$$

As opposed to the Compton process, the photon is absorbed by just a one-step process. The time scale ratio between the Compton process and the inverse bremsstrahlung is given from the last section and Eq. (7) as

$$\nu_i(\omega)\tau_C = \frac{3}{2}\frac{n_i Z_i^2}{n_e}\left(\frac{c}{v_F}\right)^3 \log\left(\frac{1}{q}\right)\frac{\omega_{pe}^2}{\omega^2}\Gamma, \tag{8}$$

where $\Gamma \sim O(c^2 k_F^2/\omega^2)$ is much larger than one from the reduction of the Compton effect due to the degeneracy. If $\nu_i(\omega)\tau_C > 1$, the inverse bremsstrahlung dominates the Compton effect. For example, when $n_e = 10^{29}$ cm^3 and $Z_i = 1$, the inverse bremsstrahlung is faster than the Compton scattering by more than a factor of 2 for a 30 keV photon. Note that

the self-burning regime identified in [2] has the electron temperature less than 30 keV, and an energetic photon from the bremsstrahlung normally have energy less than 30 keV. The inverse bremsstrahlung thereby dominates the Compton effect in our regime of interest.

Another time scale involved is the time in which an excited electron with energy E emits most of its energy by photons. This problem is dealt in [8], and the frequency is given also from Eq. (26) in [22] as $\nu_B = (n_i Z_i^2 \sigma_T c)(e^2/\hbar v_e)$. The ratio between ν_i to ν_B is $\nu_i/\nu_B = 3/2(c/v_F)^3 \log(1/q)(\omega_{pe}^2/\omega^2)(\hbar v_F/e^2)$. We note that $\nu_i/\nu_B \gg 1$ unless $\omega \gg \omega_{pe}$.

Let us summarize what we have done until now. Firstly, the Compton effect can be ignored in comparison to the inverse bremsstrahlung unless the photon frequency is much higher than the plasma frequency ($\hbar\omega_{pe} \cong 7$ keV). Secondly, a photon travels during $1/\nu_i(\omega)$ before absorbed by electrons via the inverse bremsstrahlung, and the excited electron radiates photons with various frequencies during $1/\nu_B$. These photons are absorbed by electrons again, and then re-radiated with different frequencies. Since $\nu_i/\nu_B \gg 1$ unless $\omega \gg \omega_{pe}$, the energy of photon will stay longer in the form of electron kinetic energy rather than in the form of photon energy. Especially if a photon has energy less than the plasmon ($\omega < \omega_{pe}$), the time interval in which an electron radiates via bremsstrahlung is a hundred times longer than the time interval in which a photon is absorbed via inverse bremsstrahlung. Thus, we can safely assume that, for a photon $\omega < \omega_{pe}$, the energy is instantly absorbed by electrons, and such a photon does not exist any more in the plasma. Though it is well known that a macroscopic wave cannot travel in a conventional plasma if $\omega < \omega_{pe}$, the relevance of such a property to non-correlated photons from the inverse bremsstrahlung is apparently new.

4.3. Green's function for inverse bremsstrahlung

We now address the following question: given a photon with a frequency ω_0 at the origin at t_0, how do its frequency and position evolve in time? Or what is the energy density spread $\rho(\omega, r, t : \omega_0, 0, t_0)$ as a function of position and frequency?

The photon travels a distance $\delta l_0 = c/\nu_i(\omega_0)$ in the direction of $\hat{a}_0$ and is absorbed by an electron. Let us assume that an electron does not move its position and emits the photons by the bremsstrahlung in time $\tau_B = 1/\nu_B$. Now, choose one of the photons emitted with a probability weight proportional to the energy of the photon (what we are interested in is energy not number of photons), and call it the first photon. The first photon travels the distance $\delta l_2 = c/\nu_i(\omega_1)$ in the direction of $\hat{a}_1$ and is absorbed by an electron. The electron emits the second photon and so on. After n steps, the photon position is given as

$$\delta L = c\left(\frac{1}{\nu_i(\omega_0)}\hat{a}_0 + \frac{1}{\nu_i(\omega_1)}\hat{a}_1 + \cdots + \frac{1}{\nu_i(\omega_n)}\hat{a}_n\right). \tag{9}$$

From Eq. (7), we can write the above equation as

$$\delta L = \delta l_0\left(\hat{a}_0 + \frac{\omega_1^2}{\omega_0^2}\hat{a}_1 + \frac{\omega_1^2}{\omega_0^2}\frac{\omega_2^2}{\omega_1^2}\hat{a}_2 + \cdots + \frac{\omega_1^2}{\omega_0^2}\cdots\frac{\omega_n^2}{\omega_{n-1}^2}\hat{a}_n\right). \tag{10}$$

The time taken for this whole process can be estimated as $T = n\tau_B$ from the assumption that $\nu_i/\nu_B \gg 1$. It is noted that δL is a random variable. We followed a path of the photons for which a lot of alternative paths are possible. However, by summing up many trial paths, each δL is statistically the same due to the law of large number. We thereby assume that δL represent the whole paths soundly in the statistical sense and δL is a Gaussian.

In Eq. (10), a number of random variables are involved. Firstly, $\hat{a}_i$ is the set of independent random variables which is uniform over the direction with only constraint $|\hat{a}_i| = 1$. Secondly, $g_i = \omega_i/\omega_{i-1}$ are also independent random variables, and from Eq. (36) in [8], we note that g_i is distributed uniformly in the unit interval $0 \leqslant g_i \leqslant 1$. With these consideration, it is trivial to show $\langle \delta L \rangle = 0$ and

$$\begin{aligned}\left\langle (\delta L)^2 \right\rangle &= (\delta l_0)^2\left[1 + \frac{1}{3} + \left(\frac{1}{3}\right)^2 \cdots \left(\frac{1}{3}\right)^n\right] \\ &= (\delta l_0)^2 \frac{1}{1 - (1/3)^{n+1}}.\end{aligned}$$

We can do the same analysis for $\omega_n = \omega_0(\omega_1/\omega_0)\cdots\omega_n/\omega_{n-1}$ with the result: $\langle \omega_n \rangle = \omega_0(1/2)^n$ and $\langle \omega_n^2 \rangle = \omega_0^2(1/3)^n$. Assuming δL is a Maxwellian, we obtain the Green's function ρ as

$$\begin{aligned}\rho(\omega, r, t : \omega, 0, t_0) = &\left(\frac{1}{2\pi\langle(\delta L)^2\rangle}\right)^{3/2}\left(\frac{1}{2\pi\langle\delta\omega^2\rangle}\right)^{1/2} \\ &\times \exp\left[-\frac{1}{2}\frac{r^2}{\langle(\delta L)^2\rangle} - \frac{1}{2}\frac{(\omega - \langle\omega_n\rangle)^2}{\langle\omega_n^2\rangle}\right],\end{aligned}$$

where $n \cong t/\tau_B$. The photon frequency exponentially decays with time and reach the cutoff frequency ω_{pe} quickly. We can eliminate ω in ρ by integrating ω out with the assumption that the relevant time-scale for consideration is larger than τ_B. Then, the time independent Green's function ρ is given only as a function of the position and frequency as

$$\rho_\infty(r, \omega_0) = \left(\frac{1}{2\pi(\delta l_0(\omega_0))^2}\right)^{3/2} \exp\left[-\frac{1}{2}\frac{r^2}{(\delta l_0(\omega_0))^2}\right]. \tag{11}$$

For just one-step process, the Green's function is given as

$$\rho_1(r, \omega_0) = \frac{1}{8\pi(\delta l_0(\omega_0))^3} \exp\left[-\frac{r}{\delta l_0(\omega_0)}\right]. \tag{12}$$

For an example, for a hydrogen plasma with $n_e = 10^{29}$ cm^{-3} and a photon with $\hbar\omega_0 = 30$ keV, we obtain $\delta l_0 = 10^{-5}$ cm. This is much smaller than the pellet dimension that we estimated in Section 3.

4.4. Non-local electron energy transfer equation and heat conductivity

In the previous section, the inverse bremsstrahlung has been shown to dominate the Compton effect in re-absorption mechanism for a reasonably low energy photon, and the fuel can hold the radiated energy for much longer time than we expect. This makes it necessary for us to include the re-absorption in the fuel evolution equation since most of radiations are not lost but

retained. Here, using the Green's function we derived in last section, we rewrite the full evolution equation and derive the heat conductivity.

As in Section 2.1, the evolution of the electron temperature is

$$\frac{3}{2}n_2\frac{dT_e}{dt} = P_{ie} - P_B + \eta W_F + W_d - \left(n_i Z_i^2\right)n_e B(T), \qquad (13)$$

where P_{ie} is energy input from hot ions, P_B is the bremsstrahlung losses, W_F is the fusion power and η is the fraction of energy from the fusion by-product to the electrons, and W_d is the electron heat diffusion via Coulomb collisions. From [8], the bremsstrahlung P_B is given as $P_B = K\int W(T_e,\omega)\,d\omega$, where we write explicit dependence of W on T_e from Eq. (29) in [8]. As shown in the previous section, the radiated power is retained by electrons non-locally at different locations. Thereby, P_B is no longer given by the local quantity but by an integral of the Green's function:

$$P_B(\mathbf{r}) = +\int W\left(T_e(\mathbf{r},\omega)\right)d\omega - \int\left[\int_0^\infty \rho(\mathbf{r}-\mathbf{r_1},\omega)W\left(T_e(\mathbf{r_1}),\omega\right)d\omega\right]d\mathbf{r_1}. \qquad (14)$$

As long as $\delta l_0(\omega) \ll R$ with the fuel dimension R, the bremsstrahlung is not energy-loss but diffusion. We can see readily that Eq. (13) becomes integro-differential equation, which might be intractable.

However, when $T_e(x)$ is slowly varying, the bremsstrahlung P_B in Eq. (14) has the form such as $P_B = \kappa\nabla^2 T_e$, and κ is the heat conductivity from the radiative transfer. Let us assume that the electron temperature has only linear x-dependence so that $T_e = T_0 + x(dT/dx)$, where dT/dx is very small. The energy flux through $x=0$ plane from the negative-x region to the positive-x region is

$$F^+ = +\int_0^\infty d\omega \int_{x_1<0} dx_1\,dy_2\,dz_2 \int_{x>0} dx\,dy\,dz \times\left[\rho(\mathbf{r}-\mathbf{r_1},\omega)W\left(T_e(x_1),\omega\right)\right].$$

The energy flux from the positive-x region to negative-x region, F^-, can be similarly obtained. The net flux, $F = F^- - F^+$ is then proportional to the dT/dx, whose coefficient is the heat conductivity:

$$\kappa = +2\int_0^\infty d\omega \int_{x_1>0} dx_1\,dy_1\,dz_1 \int_0^\infty da \times\left[\rho(a+x_1,y_1,z_1,\omega)\frac{\partial W}{\partial T_e}x_1\right].$$

By using ρ_1, we obtain

$$\kappa_1 = \frac{1}{2}a_1\int_0^\infty \left(\delta l_0(\omega)\right)^2\frac{\partial W}{\partial T_e}d\omega, \qquad (15)$$

where a_1 is

$$a_1 = \int_0^\infty da\int_a^\infty ds\left[\int_0^\infty dt\exp\left(-\sqrt{s^2+t^2}\right)\right]. \qquad (16)$$

By using ρ_∞, we obtain

$$\kappa_\infty = \frac{1}{2}\int_0^\infty \delta l_0(\omega)^2\frac{\partial W}{\partial T_e}d\omega. \qquad (17)$$

5. Discussion and conclusion

In summary, based on the correction of the stopping power from partial degeneracy, we show that the self-burning regime is larger than the previous result [2]. We also show that in reabsorption, the inverse bremsstrahlung dominates the Compton effect and the fuel is optically thick for bremsstrahlung losses.

These results suggest an optimal ICF regime to produce net energy using advanced aneutronic fuel. In this regime, the pellet mass is 1–20 times that of a D–T pellet, and the dimension R in compressed state is 3–8 times smaller than that of a D–T pellet. The output energy is 100–1000 MJ. The gain, defined as the ratio of the output to the total Fermi energy, is 40–200. Furthermore, since all the fusion energy resides in charged particles, the energy conversion efficiency is far better than for D–T fuels. However, unless a method for the extreme compression regime here is devised, the burning of aneutronic fuel in this regime might not be realizable. The creation of a hot spot is also problem: The hot spot must be 10 times hotter than the case of D–T. One might use a hybrid concept which uses uranium inside the pellet [23,24], or possibly chain-reaction involving D–T [3].

There are several aspects that we ignored in the computation. First, while 0D power balance equation suggests also that it may be possible to burn the D–He-3 at densities $n_e \ll 10^{28}$ cm^{-3}, the assumption that $v_F \gg V$ with V being the velocity of the fusion byproduct breaks down at $n_e \ll 10^{28}$ cm^{-3} since the proton is very energetic. Then, the stopping power will be more than that we predicted due to the velocity dependence of the stopping power [25,26]. The treatment of the ion stopping when $v_F \cong V$, however, is out of the scope of this Letter. Second, due to the degeneracy, the heat capacity of the electron gas is smaller than the classical electron gas. As ions heat partially degenerate electrons, the electrons become hot more quickly than our estimate in this Letter, which will reduce the ion stopping. Therefore, the reduced heat capacity will ease the burning condition. Third, in our simulation we included neither the particle losses in the pellet nor the radiation re-absorption. Fourth, our treatment of the relativistic effect breaks down when the electron temperature exceed 150 keV. While there exists a more rigorous theory [27], it is not computationally tractable. A valid approximation of the theory should be devised. The largest outstanding issue in this regime, however, remains a practical means for the compression and creation of the hot spot.

Acknowledgements

The authors thank R. Kulsrud, G. Hammett and S. Cohen for useful discussion. This work was supported by DOE Contract No. AC02-76CH0-3073 and by the NNSA under the SSAA Program through DOE Research Grant No. DE-FG52-04NA00139.

References

[1] J. Dawson, Fusion, vol. 2, Academic Press, New York, 1981.
[2] S. Son, N.J. Fisch, Phys. Lett. A 329 (2004) 76.
[3] S. Son, N.J. Fisch, Phys. Lett. A 337 (2005) 397.
[4] N.J. Fisch, J.M. Rax, Phys. Rev. Lett. 69 (1992) 612.
[5] N.J. Fisch, M.C. Herrmann, Nucl. Fusion 35 (1995) 1753.
[6] N.J. Fisch, M.C. Herrmann, Nucl. Fusion 34 (1994) 1541.
[7] S. Son, N.J. Fisch, Phys. Rev. Lett. 95 (22) (2005) 225002.
[8] S. Son, N.J. Fisch, Phys. Lett. A 356 (2006) 65.
[9] P.T. Leon, S. Eliezer, J.M. Martinez-Val, Phys. Lett. A 343 (2005) 181.
[10] I. Nagy, A. Arnau, P.M. Echenique, Phys. Rev. B 40 (1989) 11983.
[11] C. Gouedard, C. Deutsch, J. Math. Phys. 19 (1978) 32.
[12] I. Nagy, J. Phys. B: At. Mol. Phys. 19 (1986) L421.
[13] S. Eliezer, J.M. Martinez-Val, Laser Particle Beams 16 (1998) 581.
[14] S. Eliezer, P.T. Leon, J.M. Martinez-Val, D.V. Fisher, Laser Particle Beams 21 (2003) 599.
[15] W.M. Nevins, R. Swain, Nucl. Fusion 40 (2000) 865.
[16] M.D. Rosen, Phys. Plasmas 6 (1999) 1690.
[17] J. Dawson, C. Oberman, Phys. Fluids 5 (1962) 517.
[18] V.P. Silin, Sov. Phys. 20 (1965) 1510.
[19] J.F. Seely, E.G. Harris, Phys. Rev. A 7 (1973) 1064.
[20] Y. Shima, H. Yatom, Phys. Rev. A 12 (1975) 2106.
[21] N. Kroll, K.M. Watson, Phys. Rev. A 8 (1973) 804.
[22] J. Greene, Astrophys. J. 130 (1959) 693.
[23] T. Honda, Y. Nakao, Y. Honda, K. Kudo, H. Nakashima, Nucl. Fusion 31 (1991) 851.
[24] Y. Nakao, T. Honda, K. Kudo, Nucl. Fusion 30 (1990) 143.
[25] I. Nagy, A. Bergara, Nucl. Instrum. Methods B 115 (1996) 58.
[26] I. Nagy, B. Apagyi, Phys. Rev. A 58 (1998) R16543.
[27] B. Jancovici, Nuovo Cimento 25 (1962) 428.